Environmental Science & Technology Letters

Letter

pubs.acs.org/journal/estlcu

Soluble Fe in Aerosols Sustained by Gaseous HO_2 Uptake

Jingqiu Mao,*[,†] Songmiao Fan,[‡] and Larry W. Horowitz[‡]

[†]Geophysical Institute and Department of Chemistry and Biochemistry, University of Alaska at Fairbanks, Fairbanks, Alaska 99775-6160, United States

[‡]Geophysical Fluid Dynamics Laboratory, National Oceanic and Atmospheric Administration, Princeton, New Jersey 08540-6649, United States

Supporting Information

ABSTRACT: The soluble fraction of aerosol Fe, mainly Fe(II), represents a large source of nutrient iron to the open ocean. Fe(II) may also play an important role in the adverse health effects of ambient aerosols. Our current understanding of the reduction of Fe(III) to Fe(II) in aerosols suggests that the major pathway is the photoreduction of Fe(III)−oxalate complexes, but this pathway cannot explain the observed nighttime Fe(II) in ambient aerosols and is also limited by the supply of oxalate. Here we propose a new pathway initiated by gaseous HO_2 uptake, followed by Cu−Fe redox coupling, which can sustain nighttime Fe(II) and also dominate Fe(III) reduction in the absence of Fe(III)−oxalate complexes. Consequently, aqueous OH production is substantially enhanced via the Fenton reaction and sustained by the influx of HO_2 from the gas phase. This mechanism is potentially the major mechanism for sustaining soluble Fe(II) in ambient aerosols and can be tested by a combination of modeling and aerosol Fe speciation measurements. We hypothesize that this mechanism may also be relevant to mineral Fe dissolution in dust aerosols.

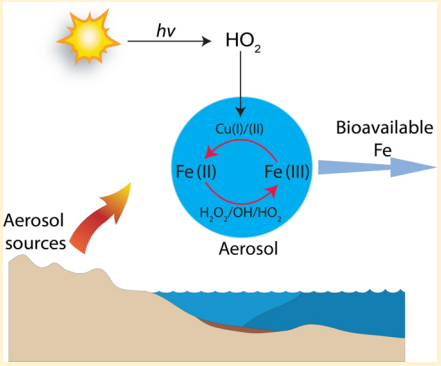

1. INTRODUCTION

Fe speciation in aerosols is of great interest for ocean biogeochemistry and public health. Fe is ubiquitous in both crustal and combustion aerosols,[1] with solubility varying greatly from ∼0.1% in soil dust to ∼80% in oil fly ash.[2] The bioavailable fraction of aerosol Fe, often assumed to consist of readily soluble Fe(II), represents a dominant source of nutrient Fe to the open ocean.[3,4] Soluble Fe in ambient aerosols may also have adverse health effects, contributing a large fraction of the oxidative potential in human lung fluid.[5] Worldwide measurements of aerosol Fe speciation suggest that a significant fraction of total dissolved Fe [Fe(II) + Fe(III)] is in the form of Fe(II), with large spatial and temporal variability (Table 1). In particular, a significant Fe(II) fraction (10−60%) was observed at night.[6−8]

Our current understanding of Fe redox cycling in aqueous aerosols is incomplete. Fe(II) can be oxidized to Fe(III) via known pathways, including its reactions with aqueous HO_2/O_2^-, OH, and H_2O_2.[9] In particular, with an atmospheric abundance of gaseous H_2O_2 (∼1 ppb and Henry's law constant of 7.4×10^4 M atm^{-1}), the chemical lifetime of Fe(II) is <1 h because of the Fenton reaction.[10]

$$Fe(II) + H_2O_2 \rightarrow Fe(III) + OH + OH^- \quad (1)$$

To sustain Fe(II) in aerosols, Fe(III) must be continuously reduced to Fe(II). This reduction is thought to be largely from the photolysis of Fe(III) organic complexes,[11−13] as the Fe(III) + HO_2/O_2^- reaction is too slow to be important. However, this photoreduction of Fe(III) cannot be responsible for the substantial fraction of nighttime Fe(II) (10−60%) observed in ambient aerosols,[6,8,14] as photons are unavailable while Fe (II) oxidation continues during the night. It also requires a large source of organic compounds to sustain the fast photolysis of Fe(III) organic complexes during the day.[15−17] Thus, there is a need for an additional reductant for Fe(III) to sustain nighttime Fe(II) and to some extent daytime Fe(II). Here we propose a new catalytic mechanism (Figure 1) that is initiated by gaseous HO_2 uptake, followed by Cu−Fe redox coupling. This mechanism may play a critical role in sustaining Fe(II) in ambient aerosols, without which soluble Fe may be rapidly converted to the insoluble form in ambient Fe-bearing aerosols, leading to a strong suppression of bioavailable Fe to the open ocean. Such a mechanism may also have important implications for quantifying adverse health effects of ambient aerosols due to the soluble form of transition metals.[5,18]

2. MATERIALS AND METHODS

2.1. Schematic. Similar to Fe, Cu is another ubiquitous component in combustion and dust aerosols.[19] Cu tends to fully dissolve at pH <5, while the solubility of Fe varies greatly from <0.1 to 80%.[20] The dissolved Cu/Fe molar ratio is mainly in the range of 0.01−0.1 (Table S1). The hydroperoxyl radical,

Received: January 11, 2017
Revised: February 1, 2017
Accepted: February 3, 2017
Published: February 3, 2017

DOI: 10.1021/acs.estlett.7b00017
Environ. Sci. Technol. Lett. 2017, 4, 98−104

Table 1. Measurements of Fractional Fe(II) (percentage) in Ambient Aerosols

location or type	Fe(II)/[Fe(II) + Fe(III)]	ref
northwest Pacific Ocean	22[a]	6
Barbados, West Indies	6–55[a]	8
Barbados, West Indies	7–28	10
North Pacific	15	39
ACE-Asia/MILAGRO/PELTI/INTEX-B field campaigns	0–73	68
tropical North Atlantic Ocean	60	69
Arabian Sea	50	70
Arabian Sea	65	71
Atlantic Ocean	38–62	72
western United States	90	73
Atlanta, GA, United States	57[a]	74
Asian outflow	33	75
subtropical northern Atlantic Ocean	5–32	76
Germany	11	77
southern Ocean and coastal Antarctica	12–100	78
St. Louis urban area	50–100	79
eastern and western United States	13–90	80

[a]Nighttime measurements were conducted and showed a significant fraction of Fe(II).

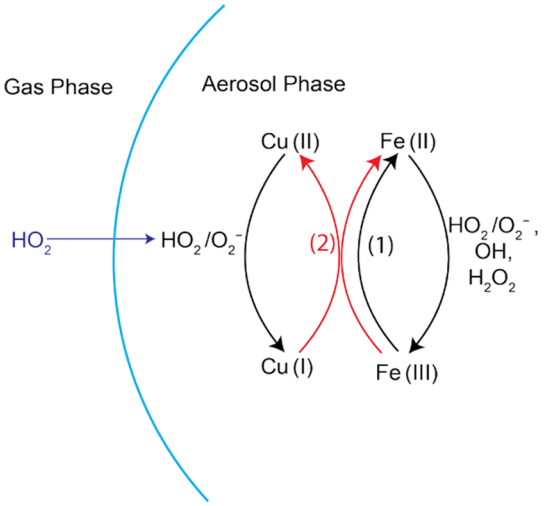

Figure 1. Schematic diagram of major Fe(III) reduction pathways in aqueous aerosols, including (1) photoreduction of Fe(III)–oxalate complexes and (2) Cu–Fe redox coupling driven by HO_2 uptake.

HO_2, is produced from atmospheric oxidation of most hydrocarbon and carbon monoxide (CO). Its daytime source, as driven by OH, tends to be stronger than nighttime sources, as driven by ozone and NO_3. Nighttime gaseous HO_2, however, can still be significant in various regions because of enhanced nighttime production.[21,22]

It is well established by laboratory measurements that gaseous HO_2 is lost rapidly to Cu-doped aerosols via the reaction[23−25]

$$Cu(II) + HO_2 \rightarrow Cu(I) + O_2 + H^+ \quad (2)$$

Within the range of Cu/Fe ratios in ambient aerosols, Cu–Fe redox coupling is expected to dominate the fate of Cu(I) and Fe(III):[26]

$$Cu(I) + Fe(III) \rightarrow Cu(II) + Fe(II) \quad (3)$$

The electron transfer reaction Cu(I) + Fe(III) is rapid with a rate constant of $1.3–3 \times 10^7$ M^{-1} s^{-1},[27−30] and this reaction can dominate the reduction of Fe(III) to Fe(II) across a wide range of Cu/Fe ratios both in aerosols and in cloud droplets.[26,31,32] The Cu–Fe redox coupling, initiated by gaseous HO_2 uptake, therefore, provides a novel catalytic pathway for reducing Fe(III) to Fe(II). As we will show below, this mechanism can potentially sustain the nighttime Fe(II) in aerosols with an ambient level of gaseous HO_2. Invoking uptake of HO_2 and conversion to H_2O by the transition metal chemistry in aerosols has been found to improve modeling of field measurements of H_2O_2.[33,34]

2.2. Fe Redox Cycling in Aerosols. To assess the diurnal variation of Fe redox cycling in aerosols, we apply a box model that accounts for the surface exchange of HO_2 and H_2O_2 between the gas phase and aerosols and computes aerosol aqueous chemistry involving OH, HO_2, H_2O_2, Cu, and Fe. The model is described in detail in ref 26. Model calculations assume an aqueous $NH_4(SO_4)_2$ aerosol with a dry radius of 0.59 μm at 85% relative humidity (RH) and 298 K. A dissolved Cu concentration of 5.9×10^{-3} M was adopted from ref 35 for background aerosols with a total Cu concentration of 3.1 ng m^{-3}, significantly lower than its concentration in the upper continental crust (~10 ng m^{-3}).[36] The dissolved Cu/Fe molar ratio is kept constant at 0.05 (approximately the mean ratio from the IMPROVE network[26]). We conduct simulations with prescribed HO_2 concentrations for noon (10 pptv) and midnight (2 pptv). Measurements of nighttime HO_2 range from 2 to 5 pptv in remote oceans[37] to >10 pptv in polluted regions.[22] The H_2O_2 concentration is assumed to be 1 ppbv in both simulations. Photolysis reactions are turned off at night. In the initial model configuration, we neglect oxalate, and its role will be addressed in the next section.

3. RESULTS AND DISCUSSION

3.1. Budget of Fe(II) in Aqueous Aerosol. Figure 2 shows the budget of dissolved Fe and $O_2(-I)$ [$\equiv HO_2(aq) + O_2^-$] in an aqueous aerosol for both noon and midnight scenarios. HO_2 is a weak acid with a pK_a of 4.7. In both scenarios, $O_2(-I)$ mainly reacts with Cu(II), producing Cu(I), which in turn reduces Fe(III) to Fe(II) via reaction 3. In contrast, the photolysis of $Fe(OH)^{2+}$ is fairly slow ($\sim 4 \times 10^{-7}$ s^{-1}) during daytime and plays a minor role in the reduction of Fe(III). This is different from aqueous chemistry in cloud droplets,[38,39] as the aqueous-phase solution in aerosols is $10^3–10^6$ times more concentrated for dissolved Cu and Fe that leads to a much stronger Cu–Fe redox coupling.

Another prominent feature is the nighttime fraction of Fe(II). As shown in Figure 2, the fraction of Fe(II) to total dissolved Fe decreases from 53% at noon to 17% at midnight, due to a decrease in the ambient level of gaseous HO_2. In fact, the fraction of nighttime Fe(II) is largely dependent on the ambient HO_2 concentration. With a higher HO_2 concentration of 4 pptv, the nighttime Fe(II) fraction can increase to 30% of total dissolved Fe. With HO_2 uptake turned off in the model, Fe(II) is completely converted to Fe(III) within several minutes. However, organic complexation of Fe(II) may slow its oxidation by the reactive oxygen species and thereby increase its fraction, which is not included in our model because of a lack of data. Therefore, both the daytime and nighttime Fe(II) in our simulations is largely sustained by gaseous HO_2 and Cu–Fe redox coupling.

DOI: 10.1021/acs.estlett.7b00017
Environ. Sci. Technol. Lett. 2017, 4, 98–104

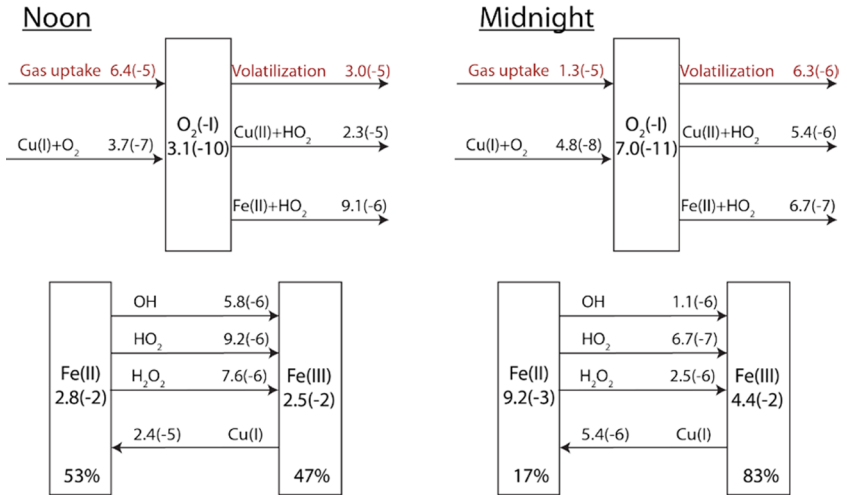

Figure 2. Simulated aerosol budgets of $O_2(-I)$ [$=HO_2(aq) + O_2^-$] and dissolved Fe in the presence of dissolved Cu, for both noon (left) and midnight (right). Only major reaction pathways are included. The values shown inside each box are aqueous concentrations (molar), with percentage numbers in the bottom panels representing the fractions of Fe(II) and Fe(III) to total dissolved Fe. The values shown above each arrow are transformation rates (molar per second). Read 6.4(−5) as 6.3×10^{-5}. Model calculations assume an aqueous $(NH_4)_2SO_4$ aerosol with a dry radius of 0.59 μm at 85% RH and 298 K. A dissolved Cu concentration of 5.9×10^{-3} M was adopted from ref 28. The dissolved Cu/Fe molar ratio is kept constant at 0.05. The aerosol pH is 1.1 with an ionic strength of 12.2 mol kg^{-1}. The gaseous HO_2 concentration is held constant at 10 pptv for noon and 2 pptv for midnight. The H_2O_2 concentration is assumed to be 1 ppbv in both simulations.

This mechanism leads to a significant and continuous production of aqueous OH via the Fe(II) + H_2O_2 reaction. We find that the aqueous OH production rate is 8.0×10^{-6} M s^{-1} for noon and 2.5×10^{-6} M s^{-1} for midnight, several orders of magnitude higher than the rate of direct uptake of gas-phase OH ($\sim 10^{-8}$ M s^{-1})[40] or nitrate and nitrite photolysis in aerosols ($\sim 10^{-9}$ M s^{-1}).[41] We find that Cu−Fe redox coupling dominates the reduction of Fe(III) to Fe(II) over a wide range of Cu/Fe ratios and pH conditions in aerosols (Figure 3). We

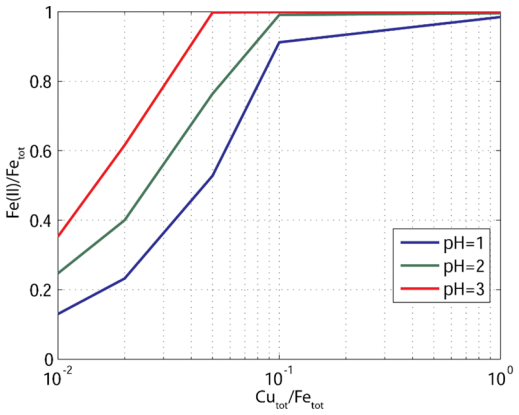

Figure 3. Simulated steady state relationship between $Fe(II)/Fe_{tot}$ and Cu/Fe_{tot} under different pH conditions for noon. The gaseous HO_2 concentration is kept at 10 pptv and the H_2O_2 concentration at 1 ppbv.

emphasize that this aqueous OH production is driven by the influx of HO_2 from ambient air, in contrast to previous laboratory measurements of the aqueous OH formation rate.[42] The conversion efficacy from gaseous HO_2 to aqueous OH depends upon the fraction of Fe(II) + H_2O_2 to total Fe(II) loss rates, which is 34% for noon and 58% for midnight (Figure 2). As gaseous HO_2 is in general far more abundant than OH,[43] this mechanism may enhance aqueous oxidation in ambient aerosols. We emphasize that this model should not be limited by sulfate aerosol but could also be applied to dust aerosols given that Cu is one of the major trace elements in crustal dust.[19] In fact, we expect that the dissolved Cu concentration in dust aerosols may be higher than currently assumed values and thus play an important role in modulating Fe speciation in dust aerosols.

3.2. Role of Oxalate in Fe Redox Cycling. We now proceed to discuss the role of oxalate in modulating Fe speciation. As the most abundant species among identified water-soluble organic compounds,[44,45] oxalate can readily form complexes with transition metal ions (TMI),[46] while formate and acetate have a much weaker tendency because of their lower complexation constants.[47] Oxalic acid ($H_2C_2O_4$) has first and second acid dissociation constants (pK_a) of 1.2 and 4.2, respectively, with stability constants (log K_{ML}) of 6.2, 3.0, and 9.4 (at zero ionic strength) for CuC_2O_4, $Fe(C_2O_4)$, and $Fe(C_2O_4)^+$, respectively.[30] Its primary sources include biomass burning and vehicle exhaust. Other sources can often be quite significant, such as in-cloud processing.[45,48]

Previous studies have shown significantly enhanced reduction of Fe(III) in the presence of oxalate.[10,49,50] This has been attributed to the photoreduction of Fe(III)−oxalate complexes in aerosols:

$$2[Fe(C_2O_4)_n]^{(3-2n)+} + h\nu \rightarrow 2Fe^{2+} + (2n-1)C_2O_4^{2-} + 2CO_2 \quad (4)$$

The photochemical lifetime of Fe(III)−oxalate complexes is rather short, on the order of minutes.[32] As oxalate is converted to CO_2, this photoreduction (reaction 4) leads to a rapid sink of oxalate.[13,16,50,51] The loss of oxalate via reaction 4 is also supported by recent field observations.[17]

To account for the role of this photoreduction process, we include oxalate complexation in the model following the method of Johnson and Meskhidze.[11] We find that Fe(III) is dominated by $Fe(C_2O_4)^+$, $Fe(C_2O_4)_2^-$, and $Fe(C_2O_4)_3^{3-}$, for assumed $C_2O_4^{2-}/SO_4^{2-}$ ratios between 0.01 and 10%, because of the high stability constant for Fe(III)−oxalate complexes.

DOI: 10.1021/acs.estlett.7b00017
Environ. Sci. Technol. Lett. 2017, 4, 98−104

The dominance of Fe(III)−oxalate complexes under these conditions is consistent with laboratory experiments.[50] In the presence of sunlight, photoreduction of Fe(III)−oxalate complexes dominates the reduction of Fe(III) to Fe(II), but this dominance decays within minutes because of the rapid depletion of oxalate, as shown by laboratory experiments.[10,51,52] To sustain this photoreduction, a large source of oxalate is thus required in the aqueous phase, on the order of 1 mM s^{-1}. This is several orders of magnitude higher than what the current understanding of oxalate production in aqueous aerosols can account for ($<10^{-3}$ mM s^{-1}).[53] Another possibility is that aerosol oxalate is not available for complexation with Fe(III), as suggested by recent measurements that the major fraction (60−80%) of aerosol oxalate is chelated with Ca, Zn, and Mg, instead of Fe.[54] We therefore conclude that the role of photoreduction of Fe(III)−oxalate complexes is likely limited by the supply of oxalate in aerosols.

3.3. Recommendations for Future Field Measurements. This new pathway for modulating Fe(II) in ambient aerosols, Cu−Fe redox coupling initiated by HO_2 uptake, may be readily examined by simultaneous measurements of dissolved Cu and Fe in ambient aerosols. Assuming a steady state for both dissolved Cu and Fe, we have $k_2[Cu(II)][HO_2] \approx k_3[Cu(I)][Fe(III)] \approx (k_5[HO_2] + k_6[H_2O_2] + k_7[HO_2])[Fe(II)]$, where k_2 and k_3 represent the reaction rate constants for reactions 2 and 3 and k_5−k_7 represent the reaction rate constants of Fe(II) with HO_2, H_2O_2, and OH, respectively. Assuming the total dissolved Cu, $[Cu]_{tot} \approx [Cu(II)]$, we have the following relationship:

$$\frac{[Fe(II)]}{[Fe]_{tot}} = \frac{k_2[HO_2]}{k_5[HO_2] + k_6[H_2O_2] + k_7[OH]} \times \frac{[Cu]_{tot}}{[Fe]_{tot}}$$

where all concentrations refer to steady state concentrations. $[Fe]_{tot}$ represents the total dissolved Fe in aerosols. Figure 3 shows the simulated steady state relationship between $Fe(II)/Fe_{tot}$ and Cu_{tot}/Fe_{tot} under different pH conditions. The linear dependence between $Fe(II)/Fe_{tot}$ and Cu_{tot}/Fe_{tot} is valid when Cu_{tot}/Fe_{tot} is <0.1. At relatively low Fe concentrations (Cu_{tot}/Fe_{tot} = 0.1−1), the Cu(I) concentration is sufficiently high to rapidly convert Fe(III) to Fe(II), resulting in a $Fe(II)/Fe_{tot}$ ratio of ∼1 and a reaction insenstive to Cu_{tot}. The pH dependence in Figure 3 is due to the reaction rate constant of the Cu(II) + O_2^- reaction being higher than that of the Cu(II) + HO_2(aq) reaction by 2 orders of magnitude and because HO_2 is a weak acid with a pK_a of 4.7 to dissociate to O_2^-. A similar relationship was also found for nighttime simulations, but Cu(I) production is decreased because of the low concentrations of gaseous HO_2. It should be noted that this relationship may vary with ambient levels of HO_2 and H_2O_2, and organic complexation for both Cu and Fe in aerosols that may largely impact their reactivity toward aqueous OH, HO_2, and H_2O_2. Field measurements must take these factors into account in an examination of this mechanism.

3.4. Relevance to Mineral Fe Dissolution. We propose a new mechanism for reducing Fe(III) to Fe(II) in ambient aerosols. This pathway, initiated by heterogeneous HO_2 aerosol uptake and followed by Cu−Fe redox coupling, can sustain nighttime Fe(II) that cannot be explained by the photoreduction of Fe(III)−oxalate complexes. We show that the photoreduction of Fe(III)−oxalate complexes is likely limited by the supply of oxalate, as this reduction consumes oxalate quickly via production of CO_2. In the absence of Fe(III)−oxalate complexation, this new reduction pathway for Fe(III) reduction during both day and night is found to sustain Fe(II) in ambient aerosols. This mechanism provides a significant source of aqueous OH that is 2 orders of magnitude stronger than direct aerosol uptake of gaseous OH and facilitates aqueous oxidation in ambient aerosols.[55] An important uncertainty in this mechanism is caused by the organic complexation in aerosols,[56] which may reduce the reactivity of Cu(II) and Fe(III) toward OH, HO_2, and H_2O_2 by several orders of magnitude.[1,57] This pathway can be tested by a combination of modeling and aerosol Fe speciation measurements. In fact, any other TMI that reacts with aqueous HO_2 may act as Cu in a similar manner and deserves further investigation.[58]

This mechanism may also be relevant to Fe dissolution in dust aerosols. As driven by atmospheric HO_2, the electron donor, Cu(I), is catalytically produced via the Cu(II) + HO_2 reaction. When a Cu(I) ion impinges on an iron oxide and donates the electron, a surficial Fe(II) locked inside an oxide lattice is formed, which leads to the release of aqueous Fe(II) and therefore a net production of bioavailable iron. While proton-promoted dissolution is relatively slow, electron donors can accelerate the dissolution process,[59] as shown in Figure 4.

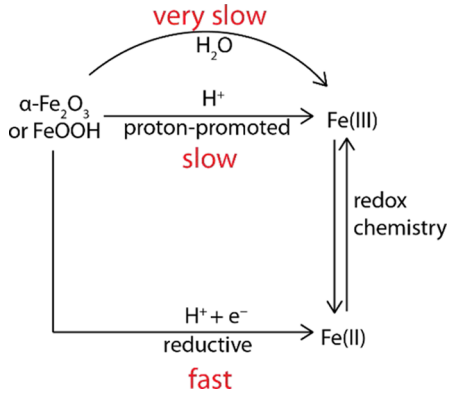

Figure 4. Different pathways of Fe dissolution, including direct dissolution, proton-promoted dissolution, and reductive dissolution. Reductive dissolution is the fastest compared to the other two, where Cu(I) may be the electron donor.

This is also consistent with field observations that suggest Fe(II) in dust aerosols is at least partly produced from reductive processes with durations on the order of 1−3 days.[60,61] In addition, this process is relatively insensitive to aerosol acidity, allowing Fe dissolution to take place at relatively high pH.[62,63] As gaseous HO_2 and dissolved Cu are readily available, Cu−Fe redox coupling would complement the Fe dissolution in acid coating of dust aerosols that is thought to be due to atmospheric processing.[39,61,64−67] The self-catalysis of Fe dissolution could increase the supply of Fe from various sources to the marine ecosystem. Future studies should aim to examine the dissolution kinetics of Fe in the presence of dissolved Cu and gaseous HO_2.

■ ASSOCIATED CONTENT

Supporting Information

The Supporting Information is available free of charge on the ACS Publications website at DOI: 10.1021/acs.estlett.7b00017.

Additional table of ambient measurements of dissolved Cu and Fe (PDF)

DOI: 10.1021/acs.estlett.7b00017
Environ. Sci. Technol. Lett. 2017, 4, 98−104

AUTHOR INFORMATION

Corresponding Author

*E-mail:jmao2@alaska.edu. Phone: +1-9074741576.

ORCID

Jingqiu Mao: 0000-0002-4774-9751

Notes

The authors declare no competing financial interest.

ACKNOWLEDGMENTS

The data and code for this paper are stored at NOAA GFDL Blue Arc File Server and can be obtained by contacting J.M. The authors thank John Dunne and Paul Ginoux at NOAA GFDL for helpful comments. J.M. and L.W.H. acknowledge NOAA Climate Program Office Grant NA13OAR4310071.

REFERENCES

(1) Jacob, D. J. Heterogeneous chemistry and tropospheric ozone. *Atmos. Environ.* **2000**, *34* (12−14), 2131−2159.

(2) Schroth, A. W.; Crusius, J.; Sholkovitz, E. R.; Bostick, B. C. Iron solubility driven by speciation in dust sources to the ocean. *Nat. Geosci.* **2009**, *2* (5), 337−340.

(3) Conway, T. M.; John, S. G. Quantification of dissolved iron sources to the North Atlantic Ocean. *Nature* **2014**, *511* (7508), 212−215.

(4) Mahowald, N. M.; Baker, A. R.; Bergametti, G.; Brooks, N.; Duce, R. A.; Jickells, T. D.; Kubilay, N.; Prospero, J. M.; Tegen, I. Atmospheric global dust cycle and iron inputs to the ocean. *Global Biogeochem. Cycles* **2005**, *19* (4), GB4025.

(5) Charrier, J. G.; Anastasio, C. On dithiothreitol (DTT) as a measure of oxidative potential for ambient particles: evidence for the importance of soluble \newline transition metals. *Atmos. Chem. Phys.* **2012**, *12* (19), 9321−9333.

(6) Buck, C. S.; Landing, W. M.; Resing, J. A.; Lebon, G. T. Aerosol iron and aluminum solubility in the northwest Pacific Ocean: Results from the 2002 IOC cruise. *Geochem., Geophys., Geosyst.* **2006**, *7* (4), Q04M07.

(7) Oakes, M.; Rastogi, N.; Majestic, B. J.; Shafer, M.; Schauer, J. J.; Edgerton, E. S.; Weber, R. J. Characterization of soluble iron in urban aerosols using near-real time data. *J. Geophys. Res.* **2010**, *115* (D15), D15302.

(8) Zhu, X.; Prospero, J. M.; Millero, F. J. Diel variability of soluble Fe(II) and soluble total Fe in North African dust in the trade winds at Barbados. *J. Geophys. Res.* **1997**, *102* (D17), 21297−21305.

(9) Jacob, D. J.; Gottlieb, E. W.; Prather, M. J. Chemistry of a Polluted Cloudy Boundary Layer. *J. Geophys. Res.* **1989**, *94* (D10), 12975−13002.

(10) Zhu, X.; Prospero, J. M.; Savoie, D. L.; Millero, F. J.; Zika, R. G.; Saltzman, E. S. Photoreduction of Iron(III) in Marine Mineral Aerosol Solutions. *J. Geophys. Res.* **1993**, *98* (D5), 9039−9046.

(11) Johnson, M. S.; Meskhidze, N. Atmospheric dissolved iron deposition to the global oceans: effects of oxalate-promoted Fe dissolution, photochemical redox cycling, and dust mineralogy. *Geosci. Model Dev.* **2013**, *6* (4), 1137−1155.

(12) Zuo, Y. Kinetics of photochemical/chemical cycling of iron coupled with organic substances in cloud and fog droplets. *Geochim. Cosmochim. Acta* **1995**, *59* (15), 3123−3130.

(13) Chen, H.; Grassian, V. H. Iron Dissolution of Dust Source Materials during Simulated Acidic Processing: The Effect of Sulfuric, Acetic, and Oxalic Acids. *Environ. Sci. Technol.* **2013**, *47* (18), 10312−10321.

(14) Fomba, K. W.; van Pinxteren, D.; Müller, K.; Iinuma, Y.; Lee, T.; Collett, J. L., Jr; Herrmann, H. Trace metal characterization of aerosol particles and cloud water during HCCT 2010. *Atmos. Chem. Phys.* **2015**, *15* (15), 8751−8765.

(15) Scheinhardt, S.; Müller, K.; Spindler, G.; Herrmann, H. Complexation of trace metals in size-segregated aerosol particles at nine sites in Germany. *Atmos. Environ.* **2013**, *74*, 102−109.

(16) Weller, C.; Tilgner, A.; Bräuer, P.; Herrmann, H. Modeling the Impact of Iron−Carboxylate Photochemistry on Radical Budget and Carboxylate Degradation in Cloud Droplets and Particles. *Environ. Sci. Technol.* **2014**, *48* (10), 5652−5659.

(17) Sorooshian, A.; Wang, Z.; Coggon, M. M.; Jonsson, H. H.; Ervens, B. Observations of Sharp Oxalate Reductions in Stratocumulus Clouds at Variable Altitudes: Organic Acid and Metal Measurements During the 2011 E-PEACE Campaign. *Environ. Sci. Technol.* **2013**, *47* (14), 7747−7756.

(18) Charrier, J. G.; Anastasio, C. Rates of Hydroxyl Radical Production from Transition Metals and Quinones in a Surrogate Lung Fluid. *Environ. Sci. Technol.* **2015**, *49* (15), 9317−9325.

(19) Schroeder, W. H.; Dobson, M.; Kane, D. M.; Johnson, N. D. Toxic trace elements associated with airborne particulate matter: a review. *JAPCA* **1987**, *37* (11), 1267−85.

(20) Deguillaume, L.; Leriche, M.; Desboeufs, K.; Mailhot, G.; George, C.; Chaumerliac, N. Transition Metals in Atmospheric Liquid Phases: Sources, Reactivity, and Sensitive Parameters. *Chem. Rev.* **2005**, *105* (9), 3388−3431.

(21) Mao, J.; Ren, X.; Zhang, L.; Van Duin, D. M.; Cohen, R. C.; Park, J. H.; Goldstein, A. H.; Paulot, F.; Beaver, M. R.; Crounse, J. D.; Wennberg, P. O.; DiGangi, J. P.; Henry, S. B.; Keutsch, F. N.; Park, C.; Schade, G. W.; Wolfe, G. M.; Thornton, J. A.; Brune, W. H. Insights into hydroxyl measurements and atmospheric oxidation in a California forest. *Atmos. Chem. Phys.* **2012**, *12* (17), 8009−8020.

(22) Mao, J.; Ren, X.; Chen, S.; Brune, W. H.; Chen, Z.; Martinez, M.; Harder, H.; Lefer, B.; Rappenglück, B.; Flynn, J.; Leuchner, M. Atmospheric oxidation capacity in the summer of Houston 2006: Comparison with summer measurements in other metropolitan studies. *Atmos. Environ.* **2010**, *44* (33), 4107−4115.

(23) Cooper, P. L.; Abbatt, J. P. D. Heterogeneous interactions of OH and HO2 radicals with surfaces characteristic of atmospheric particulate matter. *J. Phys. Chem.* **1996**, *100* (6), 2249−2254.

(24) Mozurkewich, M.; McMurry, P. H.; Gupta, A.; Calvert, J. G. Mass accommodation coefficient for HO2 radicals on aqueous particles. *J. Geophys. Res.* **1987**, *92* (D4), 4163−4170.

(25) Thornton, J. A.; Jaeglé, L.; McNeill, V. F. Assessing known pathways for HO2 loss in aqueous atmospheric aerosols: Regional and global impacts on tropospheric oxidants. *J. Geophys. Res.: Atmos.* **2008**, *113* (D5), D05303.

(26) Mao, J.; Fan, S.-M.; Jacob, D. J.; Travis, K. R. Radical loss in the atmosphere from Cu-Fe redox coupling in aerosols. *Atmos. Chem. Phys.* **2013**, *13* (2), 509−519.

(27) Bjergbakke, E.; Sehested, K.; Rasmussen, O. L. The Reaction Mechanism and Rate Constants in the Radiolysis of Fe^{2+}- Cu^{2+} Solutions. *Radiat. Res.* **1976**, *66* (3), 433−442.

(28) Hart, E. J.; Walsh, P. A molecular product dosimeter for ionizing radiations. *Radiat. Res.* **1954**, *1* (4), 342−346.

(29) Higginson, W. C. E.; Sykes, A. G. Kinetic studies of the oxidation of vanadium(III) by iron(III) in solution in aqueous perchloric acid. *J. Chem. Soc.* **1962**, 2841−2851.

(30) Sedlak, D. L.; Hoigné, J. The role of copper and oxalate in the redox cycling of iron in atmospheric waters. *Atmos. Environ., Part A* **1993**, *27* (14), 2173−2185.

(31) Deguillaume, L.; Leriche, M.; Monod, A.; Chaumerliac, N. The role of transition metal ions on HOx radicals in clouds: a numerical evaluation of its impact on multiphase chemistry. *Atmos. Chem. Phys.* **2004**, *4* (1), 95−110.

(32) Ervens, B.; George, C.; Williams, J. E.; Buxton, G. V.; Salmon, G. A.; Bydder, M.; Wilkinson, F.; Dentener, F.; Mirabel, P.; Wolke, R.; Herrmann, H. CAPRAM 2.4 (MODAC mechanism): An extended and condensed tropospheric aqueous phase mechanism and its application. *J. Geophys. Res.* **2003**, *108* (D14), 4426.

(33) Guo, J.; Tilgner, A.; Yeung, C.; Wang, Z.; Louie, P. K. K.; Luk, C. W. Y.; Xu, Z.; Yuan, C.; Gao, Y.; Poon, S.; Herrmann, H.; Lee, S.; Lam, K. S.; Wang, T. Atmospheric Peroxides in a Polluted Subtropical

DOI: 10.1021/acs.estlett.7b00017
Environ. Sci. Technol. Lett. 2017, 4, 98−104

Environment: Seasonal Variation, Sources and Sinks, and Importance of Heterogeneous Processes. *Environ. Sci. Technol.* **2014**, *48* (3), 1443−1450.
(34) Liang, H.; Chen, Z. M.; Huang, D.; Zhao, Y.; Li, Z. Y. Impacts of aerosols on the chemistry of atmospheric trace gases: a case study of peroxides and HO2 radicals. *Atmos. Chem. Phys.* **2013**, *13* (22), 11259−11276.
(35) Ross, H. B.; Noone, K. J. A numerical investigation of the destruction of peroxy radical by Cu ion catalysed reactions on atmospheric particles. *J. Atmos. Chem.* **1991**, *12* (2), 121−136.
(36) Zhang, X. Y.; Gong, S. L.; Shen, Z. X.; Mei, F. M.; Xi, X. X.; Liu, L. C.; Zhou, Z. J.; Wang, D.; Wang, Y. Q.; Cheng, Y. Characterization of soil dust aerosol in China and its transport and distribution during 2001 ACE-Asia: 1. Network observations. *J. Geophys. Res.: Atmos.* **2003**, *108* (D9), 4261.
(37) Kanaya, Y.; Sadanaga, Y.; Matsumoto, J.; Sharma, U. K.; Hirokawa, J.; Kajii, Y.; Akimoto, H. Daytime HO2 concentrations at Oki Island, Japan, in summer 1998: Comparison between measurement and theory. *J. Geophys. Res.-Atmos* **2000**, *105* (D19), 24205−24222.
(38) Siefert, R. L.; Johansen, A. M.; Hoffmann, M. R.; Pehkonen, S. O. Measurements of trace metal (Fe, Cu, Mn, Cr) oxidation states in fog and stratus clouds. *J. Air Waste Manage. Assoc.* **1998**, *48* (2), 128−143.
(39) Zhuang, G.; Yi, Z.; Duce, R. A.; Brown, P. R. Link between iron and sulphur cycles suggested by detection of Fe(n) in remote marine aerosols. *Nature* **1992**, *355* (6360), 537−539.
(40) Ervens, B.; Sorooshian, A.; Lim, Y. B.; Turpin, B. J. Key parameters controlling OH-initiated formation of secondary organic aerosol in the aqueous phase (aqSOA). *Journal of Geophysical Research: Atmospheres* **2014**, *119* (7), 3997−4016.
(41) Arakaki, T.; Kuroki, Y.; Okada, K.; Nakama, Y.; Ikota, H.; Kinjo, M.; Higuchi, T.; Uehara, M.; Tanahara, A. Chemical composition and photochemical formation of hydroxyl radicals in aqueous extracts of aerosol particles collected in Okinawa, Japan. *Atmos. Environ.* **2006**, *40* (25), 4764−4774.
(42) Shen, H.; Anastasio, C. Formation of hydroxyl radical from San Joaquin Valley particles extracted in a cell-free surrogate lung fluid. *Atmos. Chem. Phys.* **2011**, *11* (18), 9671−9682.
(43) Mao, J.; Ren, X.; Brune, W. H.; Olson, J. R.; Crawford, J. H.; Fried, A.; Huey, L. G.; Cohen, R. C.; Heikes, B.; Singh, H. B.; Blake, D. R.; Sachse, G. W.; Diskin, G. S.; Hall, S. R.; Shetter, R. E. Airborne measurement of OH reactivity during INTEX-B. *Atmos. Chem. Phys.* **2009**, *9* (1), 163−173.
(44) Mader, B. T.; Yu, J. Z.; Xu, J. H.; Li, Q. F.; Wu, W. S.; Flagan, R. C.; Seinfeld, J. H. Molecular composition of the water-soluble fraction of atmospheric carbonaceous aerosols collected during ACE-Asia. *J. Geophys. Res.* **2004**, *109* (D6), D06206.
(45) Yu, J. Z.; Huang, X.-F.; Xu, J.; Hu, M. When Aerosol Sulfate Goes Up, So Does Oxalate: Implication for the Formation Mechanisms of Oxalate. *Environ. Sci. Technol.* **2005**, *39* (1), 128−133.
(46) Okochi, H.; Brimblecombe, P. Potential Trace Metal−Organic Complexation in the Atmosphere. *Sci. World J.* **2002**, *2*, 767−786.
(47) Deguillaume, L.; Leriche, M.; Desboeufs, K.; Mailhot, G.; George, C.; Chaumerliac, N. Transition Metals in Atmospheric Liquid Phases. Sources, Reactivity, and Sensitive Parameters. *ChemInform* **2005**, *36* (49), 3388−3431.
(48) Sorooshian, A.; Varutbangkul, V.; Brechtel, F. J.; Ervens, B.; Feingold, G.; Bahreini, R.; Murphy, S. M.; Holloway, J. S.; Atlas, E. L.; Buzorius, G.; Jonsson, H.; Flagan, R. C.; Seinfeld, J. H. Oxalic acid in clear and cloudy atmospheres: Analysis of data from International Consortium for Atmospheric Research on Transport and Transformation 2004. *J. Geophys. Res.* **2006**, *111* (D23), D23S45.
(49) Faust, B. C.; Zepp, R. G. Photochemistry of aqueous iron(III)-polycarboxylate complexes: roles in the chemistry of atmospheric and surface waters. *Environ. Sci. Technol.* **1993**, *27* (12), 2517−2522.
(50) Zuo, Y.; Hoigné, J. Formation of hydrogen peroxide and depletion of oxalic acid in atmospheric water by photolysis of iron(III)-oxalato complexes. *Environ. Sci. Technol.* **1992**, *26* (5), 1014−1022.
(51) Zuo, Y.; Hoigné, J. Photochemical decomposition of oxalic, glyoxalic and pyruvic acid catalysed by iron in atmospheric waters. *Atmos. Environ.* **1994**, *28* (7), 1231−1239.
(52) Song, W.; Ma, W.; Ma, J.; Chen, C.; Zhao, J.; Huang, Y.; Xu, Y. Photochemical Oscillation of Fe(II)/Fe(III) Ratio Induced by Periodic Flux of Dissolved Organic Matter. *Environ. Sci. Technol.* **2005**, *39* (9), 3121−3127.
(53) Carlton, A. G.; Turpin, B. J.; Altieri, K. E.; Seitzinger, S.; Reff, A.; Lim, H.-J.; Ervens, B. Atmospheric oxalic acid and SOA production from glyoxal: Results of aqueous photooxidation experiments. *Atmos. Environ.* **2007**, *41* (35), 7588−7602.
(54) Furukawa, T.; Takahashi, Y. Oxalate metal complexes in aerosol particles: implications for the hygroscopicity of oxalate-containing particles. *Atmos. Chem. Phys.* **2011**, *11* (9), 4289−4301.
(55) Lin, G.; Sillman, S.; Penner, J. E.; Ito, A. Global modeling of SOA: the use of different mechanisms for aqueous-phase formation. *Atmos. Chem. Phys.* **2014**, *14* (11), 5451−5475.
(56) Zuo, Y.; Hoigné, J. Evidence for Photochemical Formation of H2O2 and Oxidation of SO2 in Authentic Fog Water. *Science* **1993**, *260* (5104), 71−73.
(57) Fan, S.-M. Photochemical and biochemical controls on reactive oxygen and iron speciation in the pelagic surface ocean. *Mar. Chem.* **2008**, *109* (1−2), 152−164.
(58) Marcus, R. A. Electron transfer reactions in chemistry. Theory and experiment. *Rev. Mod. Phys.* **1993**, *65* (3), 599−610.
(59) Martin, S. T. Precipitation and dissolution of iron and manganese oxides. *Environmental Catalysis* **2005**, 61−81.
(60) Majestic, B. J.; Schauer, J. J.; Shafer, M. M. Application of synchrotron radiation for measurement of iron red-ox speciation in atmospherically processed aerosols. *Atmos. Chem. Phys.* **2007**, *7* (10), 2475−2487.
(61) Longo, A. F.; Feng, Y.; Lai, B.; Landing, W. M.; Shelley, R. U.; Nenes, A.; Mihalopoulos, N.; Violaki, K.; Ingall, E. D. Influence of Atmospheric Processes on the Solubility and Composition of Iron in Saharan Dust. *Environ. Sci. Technol.* **2016**, *50* (13), 6912−6920.
(62) Baker, A. R.; Jickells, T. D.; Witt, M.; Linge, K. L. Trends in the solubility of iron, aluminium, manganese and phosphorus in aerosol collected over the Atlantic Ocean. *Mar. Chem.* **2006**, *98* (1), 43−58.
(63) Hand, J. L.; Mahowald, N. M.; Chen, Y.; Siefert, R. L.; Luo, C.; Subramaniam, A.; Fung, I. Estimates of atmospheric-processed soluble iron from observations and a global mineral aerosol model: Biogeochemical implications. *J. Geophys. Res.* **2004**, *109* (D17), D17205.
(64) Sedwick, P. N.; Church, T. M.; Bowie, A. R.; Marsay, C. M.; Ussher, S. J.; Achilles, K. M.; Lethaby, P. J.; Johnson, R. J.; Sarin, M. M.; McGillicuddy, D. J. Iron in the Sargasso Sea (Bermuda Atlantic Time-series Study region) during summer: Eolian imprint, spatio-temporal variability, and ecological implications. *Global Biogeochem. Cycles* **2005**, *19* (4), GB4006.
(65) Edwards, R.; Sedwick, P. Iron in East Antarctic snow: Implications for atmospheric iron deposition and algal production in Antarctic waters. *Geophys. Res. Lett.* **2001**, *28* (20), 3907−3910.
(66) Fan, S.-M.; Moxim, W. J.; Levy, H., II Aeolian input of bioavailable iron to the ocean. *Geophys. Res. Lett.* **2006**, *33* (7), L07602.
(67) Ito, A. Atmospheric Processing of Combustion Aerosols as a Source of Bioavailable Iron. *Environ. Sci. Technol. Lett.* **2015**, *2* (3), 70−75.
(68) Takahama, S.; Gilardoni, S.; Russell, L. M. Single-particle oxidation state and morphology of atmospheric iron aerosols. *J. Geophys. Res.* **2008**, *113* (D22), D22202.
(69) Johansen, A. M.; Siefert, R. L.; Hoffmann, M. R. Chemical composition of aerosols collected over the tropical North Atlantic Ocean. *Journal of Geophysical Research: Atmospheres* **2000**, *105* (D12), 15277−15312.
(70) Johansen, A. M.; Hoffmann, M. R. Chemical characterization of ambient aerosol collected during the northeast monsoon season over

DOI: 10.1021/acs.estlett.7b00017
Environ. Sci. Technol. Lett. 2017, 4, 98−104

the Arabian Sea: Labile-Fe(II) and other trace metals. *J. Geophys. Res.* **2003**, *108* (D14), 4408.
(71) Siefert, R. L.; Johansen, A. M.; Hoffmann, M. R. Chemical characterization of ambient aerosol collected during the southwest monsoon and intermonsoon seasons over the Arabian Sea: Labile-Fe(II) and other trace metals. *J. Geophys. Res.* **1999**, *104* (D3), 3511−3526.
(72) Trapp, J. M.; Millero, F. J.; Prospero, J. M. Trends in the solubility of iron in dust-dominated aerosols in the equatorial Atlantic trade winds: Importance of iron speciation and sources. *Geochem., Geophys., Geosyst.* **2010**, *11* (3), Q03014.
(73) Upadhyay, N.; Majestic, B. J.; Herckes, P. Solubility and speciation of atmospheric iron in buffer systems simulating cloud conditions. *Atmos. Environ.* **2011**, *45* (10), 1858−1866.
(74) Oakes, M.; Weber, R. J.; Lai, B.; Russell, A.; Ingall, E. D. Characterization of iron speciation in urban and rural single particles using XANES spectroscopy and micro X-ray fluorescence measurements: investigating the relationship between speciation and fractional iron solubility. *Atmos. Chem. Phys.* **2012**, *12* (2), 745−756.
(75) Moffet, R. C.; Furutani, H.; Rödel, T. C.; Henn, T. R.; Sprau, P. O.; Laskin, A.; Uematsu, M.; Gilles, M. K. Iron speciation and mixing in single aerosol particles from the Asian continental outflow. *J. Geophys. Res.: Atmos.* **2012**, *117* (D7), D07204.
(76) Chen, Y.; Siefert, R. L. Seasonal and spatial distributions and dry deposition fluxes of atmospheric total and labile iron over the tropical and subtropical North Atlantic Ocean. *J. Geophys. Res.* **2004**, *109* (D9), D09305.
(77) Dedik, A. N.; Hoffmann, P.; Ensling, J. Chemical characterization of iron in atmospheric aerosols. *Atmos. Environ., Part A* **1992**, *26* (14), 2545−2548.
(78) Gao, Y.; Xu, G.; Zhan, J.; Zhang, J.; Li, W.; Lin, Q.; Chen, L.; Lin, H. Spatial and particle size distributions of atmospheric dissolvable iron in aerosols and its input to the Southern Ocean and coastal East Antarctica. *J. Geophys. Res.: Atmos.* **2013**, *118* (22), 2013JD020367.
(79) Majestic, B. J.; Schauer, J. J.; Shafer, M. M.; Turner, J. R.; Fine, P. M.; Singh, M.; Sioutas, C. Development of a Wet-Chemical Method for the Speciation of Iron in Atmospheric Aerosols. *Environ. Sci. Technol.* **2006**, *40* (7), 2346−2351.
(80) Siefert, R. L.; Webb, S. M.; Hoffmann, M. R. Determination of photochemically available iron in ambient aerosols. *J. Geophys. Res.* **1996**, *101* (D9), 14441−14449.

DOI: 10.1021/acs.estlett.7b00017
Environ. Sci. Technol. Lett. 2017, 4, 98−104